

SYNCHROTRON SAXS CHARACTERIZATION OF NANOPARTICLES ASSEMBLED AT THE LIQUID-AIR INTERFACE

Pharunee SARMPHIM¹, Siriwat SOONTARANON², Chitnarong SIRISATHITKUL³, Krit KOYVANICH⁴, Komkrich CHOKPRASOMBAT⁵

Small angle X-ray scattering (SAXS) has been used to characterize nanoparticles, normally in forms of colloidal suspension. In this study, FePt₃ nanoparticles were self-assembled at the liquid-air interface, transferred to SiO-coated copper grids and then measured by synchrotron SAXS. The scattering profile displays a single broad peak. The scattering vector at which this peak occurs (q_{peak}) varies with the concentration of FePt₃ colloidal suspension used in the liquid-air interface assembly. When the concentration is increased from 0.2 to 0.4 mg/ml, the q_{peak} is decreased signifying the increase in particle spacing. The result is consistent with transmission electron microscope (TEM) images that the voids in self-assembly pattern are increasingly observed at higher concentrations used.

Keywords: FePt₃ nanoparticles, small angle X-ray scattering, self-assembly, liquid air interface.

1. Introduction

Properties of nanoparticles are primarily governed by their size and shape. For the application in forms of nanoparticle assembly, the variation in collective properties is not only due to the individual morphology but also their arrangement [1]. Several methods including Langmuir-Blodgett and liquid-air interface assembly have been used to regulate the nanoparticle assembly and resulting patterns are routinely inspected by transmission electron microscope (TEM). Other characterizations are also needed to complement TEM images of limited areas [2-7]. Like dynamic light scattering (DLS) [2-4], small angle X-ray scattering (SAXS) has normally been used with nanoparticles suspended in carrier liquids [5-7]. In addition to particle size distribution, SAXS is able to characterize the periodicity of nanostructure. So far, such works are mostly applied to macromolecules [8,9].

¹ Walailak University, Thailand, email: s.pharunee.y@gmail.com

² Synchrotron Light Research Institute, Thailand, email: siriwat.sn@gmail.com

³ Walailak University, Thailand, corresponding author, email: chitnarong.siri@gmail.com,

⁴ Prince of Songkla University, Thailand, email: krit_com@hotmail.com

⁵ Thaksin University, Thailand, email: komkrich28@gmail.com

When X-ray is scattered at nanoparticle assembly, the amplitude of interference intensity on each detection plane depends on the orientation and distance of the particle relative to each other. The particle arrangement gives rise to the characteristic 2D interference pattern, when measured in a circle around the primary beam. The scattering intensity is usually presented as a function of the scattering vector (q) which is a difference between scattered and incoming wave vector. The scattering angle (2θ) and X-ray wavelength (λ) are related to this q as;

$$q = \frac{4\pi \sin \theta}{\lambda} \quad (1)$$

When nanostructured assembly is highly ordered and periodic, the distance between aligned particles (d), also known as d -spacing, can be determined from the scattering vector at which the SAXS peak occurs (q_{peak}) [8].

$$d = \frac{2\pi}{q_{peak}} \quad (2)$$

In this study, SAXS profiles of dried nanoparticles on TEM grid substrates obtained by the direct dropping and the self-assembly at the liquid-air interface were compared. Superparamagnetic iron-platinum (FePt_3) is selected for this characterization because its conversion to ferromagnets after heat treatment is primed for data and energy storage [10,11].

2. Materials and Methods

FePt_3 nanoparticles suspended in hexane were synthesized by using the procedure detailed in the published article [12]. Samples in two forms, i.e. drying droplet and monolayer self-assembled at the liquid-air interface, were characterized. The drying droplets were obtained by dropping FePt_3 colloidal suspensions directly on carbon-coated copper grids. The precursors in the synthesis were also investigated by comparing Sample 1 (prepared by using $\text{Fe}(\text{acac})_3$) and Sample 2 (prepared by using $\text{Fe}(\text{hfac})_3$). For the self-assembly at the liquid-air interface, the method followed that proposed by Dong et al. [13]. FePt_3 colloidal suspensions was dropped on the diethylene glycol (DEG) and then transferred to SiO -coated copper grids. The concentration of colloidal suspensions synthesized by using $\text{Fe}(\text{dbm})_3$ were diluted to three different concentrations, i.e. 0.2, 0.3 and 0.4 mg/mL, respectively referred to as Samples A, B, and C. All samples were dried at room temperature before characterization. TEM images were obtained by using JEOL, JEM-2010 and FEI, Tecnai G² 20 with 200 kV accelerating voltage.

In the SAXS experiment at BL1.3W of Synchrotron Light Research Institute (Public organization) Thailand [14], each sample was installed on an aluminum frame at 1475.8 mm away from a CCD detector (Mar SX165). The

silver behenate powder was measured to align of the measured patterns and calibrate the sample-detector distance. The signal from empty frame and grid substrate were also collected as references. Each sample was exposed for 300 s, in which the maximum recorded intensity was close to saturate the detector. The scattering patterns were recorded and normalized with an integrated incident beam intensity measured by an ionization chamber. The sample transmissions were corrected using the measured beam intensity after the sample from a photodiode installed in front of the beam stop. The SAXS intensity plots against q were finally obtained after background subtraction and circular averaging.

3. Results and Discussion

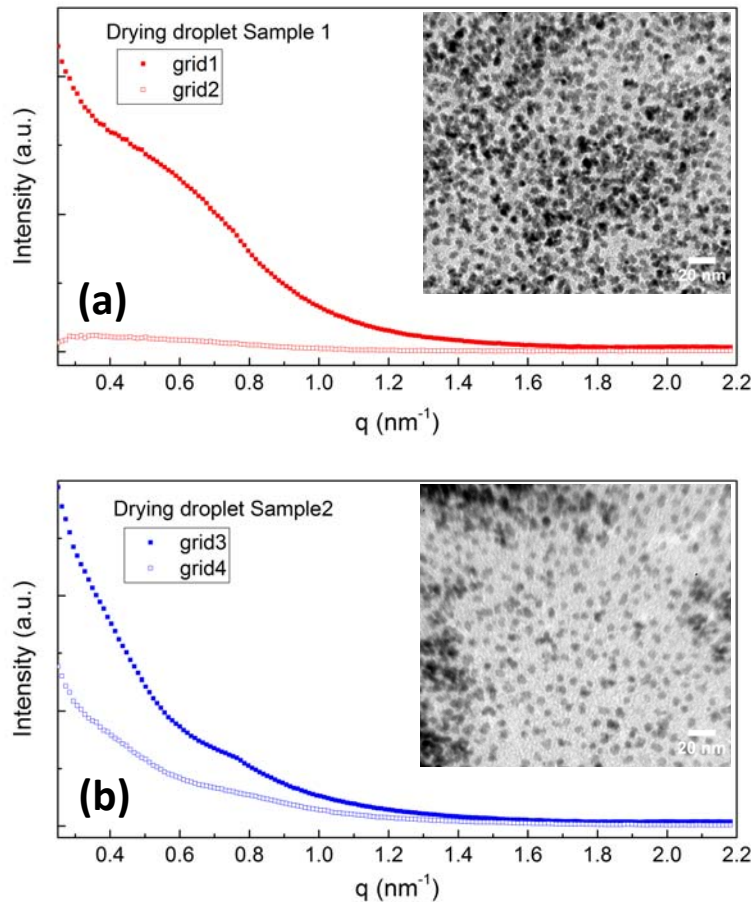


Fig. 1. SAXS scattering profiles from drying droplets of Samples (a) 1 and (b) 2. Their TEM images are shown in the inset.

In Fig. 1, SAXS intensity profiles of drying droplets exhibit the decrease with the increase in q before reaching the saturation around 1.5 nm^{-1} . With increasing q , the decrease in slopes particularly marked in Sample 2 is an opposite trend to that measured in forms of nanoparticles suspended in carrier liquids [7]. The difference between Samples 1 and 2 is attributed to the different size and spatial distributions shown by TEM insets. Nanoparticles in Sample 1 have averagely smaller diameter and particle spacing. In both samples, particles do not spread into monolayers but agglomerate on some parts of TEM grids. Interestingly, the intensity is greatly varied when the measurement is repeated on two grids from the same sample. While some features are similar, the SAXS intensities are not comparable between grids 1 and 2 from Sample 1 in Figure 1(a) as well as between grids 3 and 4 from Sample 2 in Figure 1(b). This irreproducibility emphasizes the influence of particle arrangement on SAXS profiles since the patterns of drying droplets from the same sample of similar size distribution are highly diverse.

SAXS profiles of monolayers assembled at DEG-air interface in Figure 2 have contrast characteristics to those of drying droplets. Instead of the monotonic decrease in SAXS intensity, all samples from three different concentrations display single broad peaks locating around $q = 1 \text{ nm}^{-1}$. Whereas the SAXS intensities in the case of two grids from the same sample are not reproducible, the peak remains at the comparable position. Apparently, the peak position is solely dependent on the pattern of monolayer obtained from the varying concentrations of FePt_3 colloidal suspension.

SAXS profiles around q_{peak} are magnified for further analysis as exemplified in Figure 3. The q_{peak} is clearly shifted to a lower value when the concentration of FePt_3 colloidal suspension is increased from 0.2 to 0.4 mg/mL. It follows that the d -spacing in Table 1, calculated from q_{peak} following Eq. (2), is increased with this concentration. The results indicate larger distances between two particles in the case of the higher concentrations. This finding agrees well with TEM images and the published articles [12] that the particle spacing is approximately 6 nm, slightly larger than particle diameter. Also, the voids are increasingly observed with increasing concentrations used in the liquid-air interface assembly.

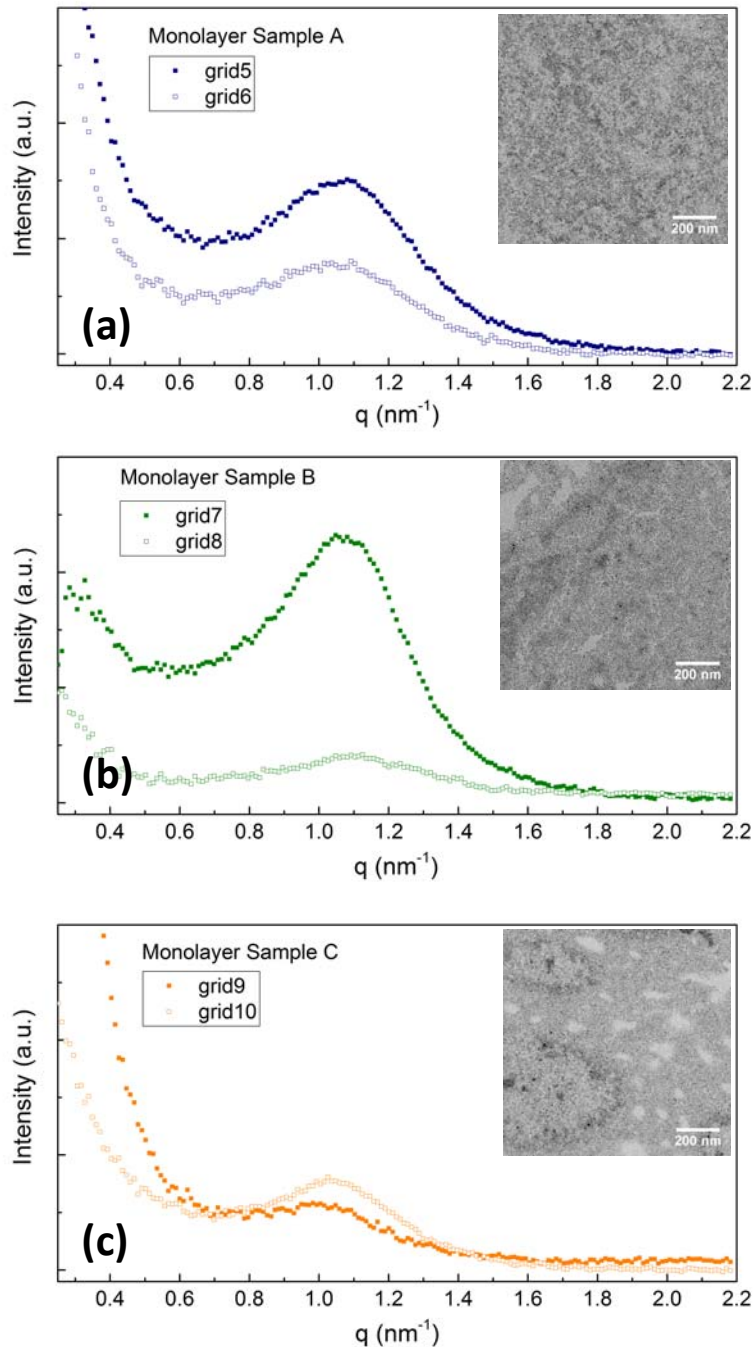


Fig. 2. SAXS scattering profiles from nanoparticles assembled at the liquid-air interface using (a) 0.2 (b) 0.3 (c) 0.4 mg/mL. Their TEM images are shown in the inset

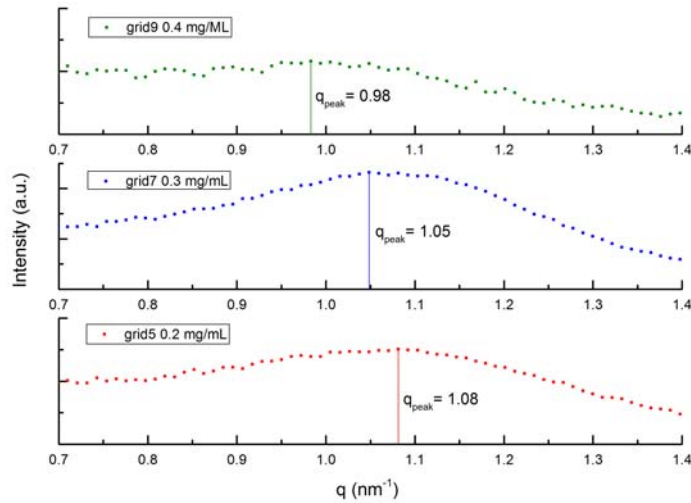


Fig. 3. Variation in position of SAXS peaks with the concentration of colloidal suspension in liquid-air interface assembly

Table 1

Variations of q_{peak} and average d -spacing with the concentration of FePt_3 colloidal suspension in the liquid-air interface assembly.

Sample	Concentration (mg/mL)	q_{peak} (nm^{-1})	d (nm)
A	0.2	1.08	5.78 ± 0.03
		1.09	
B	0.3	1.05	5.79 ± 0.20
		1.12	
C	0.4	0.98	6.26 ± 0.13
		1.03	

4. Conclusions

This study demonstrates that synchrotron SAXS cannot only be used in morphological characterization but also the arrangement of FePt_3 nanoparticle assembly. The liquid-air interface assembly enabled more control on nanoparticle arrangement. In contrast to drying droplets, the SAXS profiles exhibited the broad peak in the case of nanoparticles assembled at the DEG-air interface. The position of such peak was varied with the concentration of FePt_3 colloidal suspension used in the liquid-air interface assembly. The particle spacing computed from the position of SAXS peak was in good agreement with TEM imaging.

Acknowledgements

This work is financially supported by Walailak University (Grant no. WU59121). The authors would like to thank K. Ratchaphonsaenwong of Kon Khaen University and B. Chayasombat of National Metals and Materials Technology Center for their assistance in TEM imaging.

R E F E R E N C E S

- [1]. *M. A. Neouze*, “Nanoparticle assemblies: main synthesis pathways and brief overview on some important applications”, *J. Mater. Sci.*, **vol. 48**, 2013, pp. 7321-7349.
- [2]. *J. K. Lim, S. P. Yeap, H. X. Che, and S. C. Low*, “Characterization of magnetic nanoparticle by dynamic light scattering”, *Nanoscale Res. Lett.*, **vol. 8**, 2013, article ID 381.
- [3]. *C. Nadejde, E. Puscasu, F. Brinza, L Ursu, D. Creanga, and C. Stan*, “Preparation of soft magnetic materials and characterization with investigation methods for fluid samples”, *U. P. B. Sci. Bull. Ser. A*, **vol. 77**, 2015, pp. 277-284.
- [4]. *S. Gopinath, and J. Philip*, “Preparation of metal oxide nanoparticles of different sizes and morphologies, their characterization using small angle X-ray scattering and study of thermal properties”, *Mater. Chem. Phys.*, **vol. 145**, 2014, pp. 213-221.
- [5]. *H. Borchert, E.V. Shevehenko, A. Robert, I. Mekis, A. Kornowski, G. Grubel, and H. Weller*, “Determination of nanocrystal sizes: A comparison of TEM, SAXS, and XRD studies of highly monodisperse CoPt₃ particles”, *Langmuir*, **vol. 21**, 2005, pp. 1931-1936.
- [6]. *X. Chen, J. Schroder, S. Hauschild, S. Rosenfeeldt, M. Dulle, and S. Forster*, “Simutaneous SAXS/WAXS/UV-Vis study of the nucleation theory”, *Langmuir*, **vol. 31**, 2015, pp. 11678-11691
- [7]. *K. Chokprasombat, K. Koyvanich, C. Sirisathitkul, P. Harding, and S. Rungmai*, “Investigation of surfactant effect on size distribution of FePt-based nanoparticles by synchrotron SAXS and TEM”, *Trans Ind. Inst. Met.*, **vol. 69**, 2016, pp. 733-740.
- [8]. *D. Togashi, I. Otsuka, R. Borsali, K. Takeda, K. Enomoto, S. Kawaguchi, and A. Narumi*, “Maltopentaose-conjugate CTA for RAFT polymerization generating nanostructured bioresource-block copolymer”, *Biomacromolecules*, **vol. 15**, 2014, pp. 4509-4519.
- [9]. *S. Skou, R. E. Gillilan and N. Ando*, “Synchrotron-based small-angle X-ray scattering of protein in solution”, *Nature Protocols*, **vol. 9**, no. 7, 2014, pp. 1727-1739.
- [10]. *Y. Liu, Y. Jiang, X. Zhang, Y. Wang, Y. Zhang, H. Liu, H. Zhai, Y. Liu, J. Yang, and Y. Yan*, “Structural and magnetic properties of the ordered FePt₃, FePt and Fe₃Pt nanoparticles”, *J. Solid State Chem.*, **vol. 209**, 2014, pp. 69-73.
- [11]. *K. Chokprasombat*, “Synthesis of patterned media by self-assembly of FePt nanoparticles”, *Walailak J. Sci. & Tech.*, **vol. 8**, 2011, pp. 87-96.
- [12]. *P. Sarmphim, K. Chokprasombat, C. Sirisathitkul, Y. Sirisathitkul, K. Ratchaphonsaenwong, S. Pinitsoontorn, and P. Harding*, “Liquid-air interface self-assembly of nanoparticles synthesized from reaction between Fe(dbm)₃ and Pt(acac)₂”, *J. Clust. Sci.*, **vol. 27**, 2016, pp. 1-8.
- [13]. *A. Dong, J. Chen, P. M. Vora, J. M. Kikkawa, and C. B. Murray*, “Binary nanocrystal superlattice membranes self-assembled at the liquid-air interface”, *Nature*, **vol. 466**, 2010, pp. 474-477.
- [14]. *S. Soontaranon, and S. Rungmai*, “Small angle X-ray scattering at Siam Photon Laboratory”, *Chin. J. Phys.*, **vol. 50**, 2012, pp. 204-210.